

*Full Length Research Paper*

# Monitoring the temperature of the milling process using infrared camera

Carlos Henrique Lauro, Lincoln Cardoso Brandão\* and Sergio Luiz Moni Ribeiro Filho

Department of Mechanical Engineering, Federal University of São João del-Rei, Praça Frei Orlando, 170, São João del-Rei, CEP 36307-352.

Accepted 17 June, 2013

The study of temperatures generated in machining processes has been the theme of research since the beginning of the XX century. High temperatures can provoke changes in the microstructure of materials, resulting in form errors that may cause loss of the machined material and a decrease of tool life. As a result, high temperatures can be responsible an increase in production costs. This work uses a methodology to select the machining parameters in order to define the best parameters of influence for decreasing temperature during the milling of aluminum alloys. Work pieces were milled using a carbide end mill without coolant fluid. The experimental factors were feed rate, cutting speed, radial depth of cut and cutting direction. An infrared camera was used to capture the temperature on the opposite face of the cutting region, consequently allowing the monitoring of the temperature range during the cutting process. The results showed that the increase in temperature has a direct relation with the radial depth of cut, feed rate and cutting direction. Furthermore, the use of the infrared camera during the milling process showed flexibility and easy data acquisition.

**Key words:** Milling, thermograph, temperature, aluminum alloys, feed rate.

## INTRODUCTION

Aluminum and its alloys are among the materials currently used in the mechanical industry, mainly because of their resistance to oxidation. This occurs because the atoms on its surface react with oxygen, which generates an oxide layer preventing the deterioration of the material. Moreover, aluminum has low density, corresponding to 1/3 of steel, good formability, and the capability of being employed in several designs. Aluminum is used for the production of equipment that requires mechanical strength with low strain, and which generally needs to be light weight, in specific application such as; cars, motorcycles, bikes, furniture, and airplanes. The greater part of an airplane's structure uses 7000 grade aluminum alloys because it combines great strength with light weight and milling is the main manufacturing process.

According to Davim and Correia (2006), another

characteristic of aluminum is its great machining capability because it has the lowest energy consumption per volume of material. Among the machining processes, milling has a lot of applications in industries across the world, but it is very complex since it needs to remove great quantities of material while simultaneously producing complex surfaces. However, it generates components with excellent quality, accuracy, and flexibility. Milling is used in the production of such parts as plane surfaces, grooves, pockets, undefined profiles, and others (Zaghbani and Songmene, 2009).

Within the framework of optimizing the machining process, understanding the temperature that occurs during the milling is essential. According to Le Coz et al. (2012), the main difficulties in measuring cutting temperature during milling occurs because: (a) the tool is rotating and regularly entering and leaving the work

\*Corresponding author. E-mail: [lincoln@ufsj.edu.br](mailto:lincoln@ufsj.edu.br).

piece; (b) the zone affected by the heat moves on the work piece surface, and (c) the chips may hinder the measurement. Moreover, the methods to define the percentage of energy that goes into tool, chip, and work piece vary and depend on each machining, where the main objective is to know the percentage of energy to improve the tool's quality. Nowadays, infrared cameras are commonly used to measure the temperature distribution on machined surfaces. Materials with temperatures above 0 Kelvin show electromagnetic waves. Temperature will therefore increase the spectrum of emitted wavelength moving short wavelengths. So the infrared camera measures the intensity of infrared radiation in the measurement area of the camera (May et al., 2012).

According to Brandão et al., (2008), a great volume of work has been performed on thermal modeling aiming to understand the heat flux in machining processes. The most frequently used methodologies for defining the heat flux in machining processes are finite element techniques and the inverse heat conduction method. The research has focused on the modeling of the shear zone and several studies were developed using finite element techniques applying Abaqus<sup>TM</sup>, ANSYS<sup>TM</sup>, MARC<sup>TM</sup> and other software (Maranhão and Davim, 2010). The simulation techniques can be said to be suitable for the modeling of heat transfer in machining processes by mapping tool isotherms with the assumption of a uniform plane heat flux profile (Çolak, 2012). When the inverse heat conduction method is considered, the use of this technique depends on knowing the temperature in the cutting region, and as a rule, it is necessary to embed a thermocouple in the work piece to monitor the temperature in loco during the experiments (Luchesi and Coelho, 2012).

Thermography is an easy to use technique because it permits the monitoring of temperatures in the cutting region in simple processes, such as turning and milling, and in more complex processes, such as drilling and tapping. It can define the tool wear, the efficiency of the process, and the quality of the products minimizing burr formation, for example (Chern, 2006). Dörr et al., (2003) have also monitored the machining process. They used an infrared camera, assembled on the opposite face of the drill entrance, to monitor the drilling process. Uncoated drills and ones with coatings of (TiAl)N, TiAlBON and (TiAl)N + ZrO<sub>2</sub> were used to evaluate the influence of friction on the process. The results show high temperatures for uncoated drills reaching 908°C. The lowest values of 35°C they found for drills with (TiAl)N + ZrO<sub>2</sub> coatings. The infrared camera was able to help define the best coating for the drilling process without interfering directly in the process.

According to Sutter et al. (2003), the infrared camera can show a heat point near the cutting zone. The size of this point can range from 300 to 350 µm on the tool/work piece interface, which corresponds to 2/3 of the used

depth of cut. Their work has shown that the temperature increases with the cutting speed. Temperature values of 82°C in the shear zone during chip formation demonstrated the accuracy of the technique, which does not require complex calibrations and thermocouples to be embedded in the work piece.

Biermann and Heilmann (2010) monitored the temperature in the milling of the aluminum alloy (Al/Si/Mg/Mn). According to the authors, the surface temperatures occurring in milling using different cooling showed that the cooling does not significantly affect the cutting zone and chip temperatures. Furthermore, the authors support that the advantages to this cooling strategy can be considered in face milling of complex-shaped work pieces. Davoodi and Hosseinzadeh (2012) used an infrared system to monitor temperature in plane milling. According to the authors, the infrared sensor must be installed as close as possible to the desired surface. The results showed that the main gains are: a high response rate, an ability to measure temperature at a distance from the cutting zone, no holes in the tool or work piece to install the instruments are needed, and the technique can be used for all types of materials.

It can therefore be stated that the infrared camera allows us to monitor the temperature of the machining process with accuracy and that it also assists us with the choice of cutting parameters, tool selection and coating. The methodology is easy to use because the response parameters appear on a color map with the temperature range without conversion systems or indirect data analysis. The monitoring of temperature allows you to know and avoid changes in microstructures, residual stress, and, consequently, surface cracks that occur with thermal contractions. Finally, the use of an infrared camera in all machining processes can show temperature ranges according to the machined materials, avoiding the insertion of thermocouples or other devices for monitoring temperature.

## MATERIALS AND METHODS

A series of trials were carried out on work pieces of 100 × 38 × 8 millimeters of aluminum 7050 with the chemical composition according to Table 1. Tests used an end mill model R216.33-20040-AC38U CoroMill® Plura with 20 mm of diameter, length of 104 mm, depth of cut (DOC<sub>MAX</sub>) of 38 mm, and number of flutes of 3. All machining trials were conducted on a ROMI Discovery 560 machining center of 10,000 rpm and a drive motor of 12.5 kW.

The milling strategy left a wall with a 2 mm thickness that allowed for the measurement of the temperature on the opposite side of the cutting region using two radial depths of cut (ae), as shown in Figure 1. The first milling strategy milled a depth of cut of 6 millimeters at once, and the second milling strategy removed 2 mm. Preliminary tests prepared the work piece for the second condition, maintaining the work piece wall at 4 mm of thickness and allowing a depth of cut of 2 mm. The complete sequence of tests occurred after cooling of the work piece, avoiding the influence of heat generated in preparatory tests.

The parameters used to generate the variation of temperature during the milling tests were a feed rate of 0.10 to 0.25 m/rev and a

**Table 1.** Chemical composition of 7050 aluminum alloy (%weight).

	Cr	Cu	Fe	Mg	Mn	Si	Zn	Zr	Ti	Al
Min.	-	1.5	-	-	-	-	5.70	0.10	-	Balance
Max.	0.04	2.6	0.15	2.60	0.10	0.12	6.70	0.15	0.06	Balance

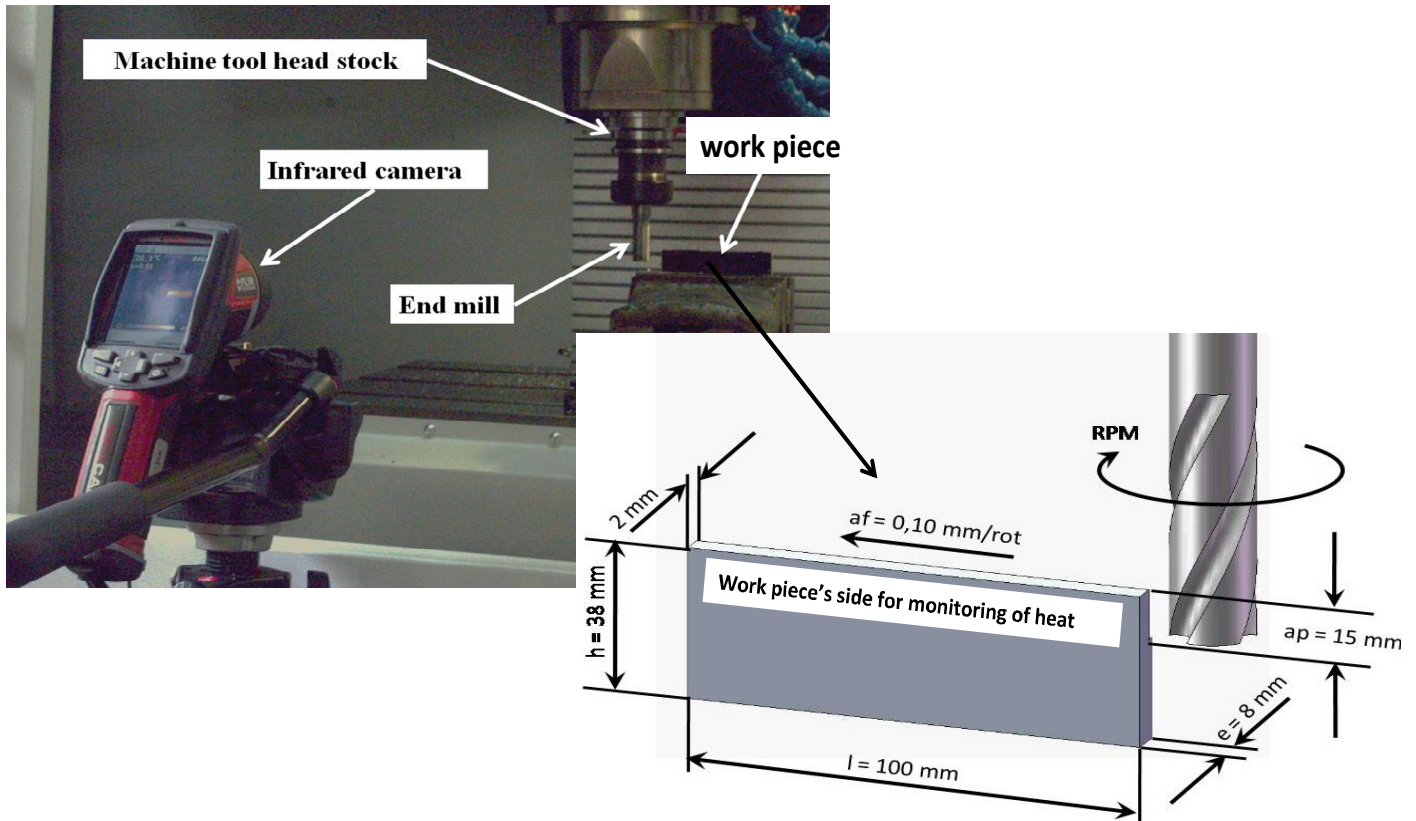


**Figure 1.** Assembly of the infrared camera with detail of work piece.

cutting speed of 314 to 628 m/min, according to the supplier of the tool. The axial depth of cut was kept constant at 15 mm. The milling experiments were carried out in dry cutting conditions in order to increase the temperature and generate high heat flux. The work pieces were painted black due to the low emissivity of aluminum. Figure 1 shows the setup of experiments and a detail of the work piece's dimensions. The data acquisition of temperature was done using a FLIR infrared camera model SYSTEMS, with an accuracy of 0.1°C. The assembly of the infrared camera was kept constant at 840 mm from the heat source.

**RESULTS**

With the experiment assembly shown in Figure 1, temperature curves were recorded on at least three positions of the work piece along the length of the work piece, as can be seen in Figure 2. The data acquisition was based on thermograms that depended exclusively on

the feed rate and the number of thermograms recorded, which varied from three to five. Thus, it was possible to obtain five thermograms using a feed rate of 0.10 mm/rev with a more accurate variation of temperature, and only three thermograms for the feed rate of 0.25 mm/rev. However, in spite of the number of thermograms for 0.25 mm/rev being three, it was possible to observe the tendency of the temperature to increase with the end mill movement in the feed direction.

At the bottom of Figure 2(a) a color map can be observed with a temperature range of 21 to 30°C and a peak of 24.8°C in the upper left corner. The first temperatures ranges were recorded at 15 mm from the work piece's left border. The heat flux precedes the end mill with a temperature peak of 74.4°C with a temperature range of 23 to 61°C in the middle of the work piece, Figure 2(b). The last temperature range occurred on the end of the work piece at 15 mm of the work piece's right

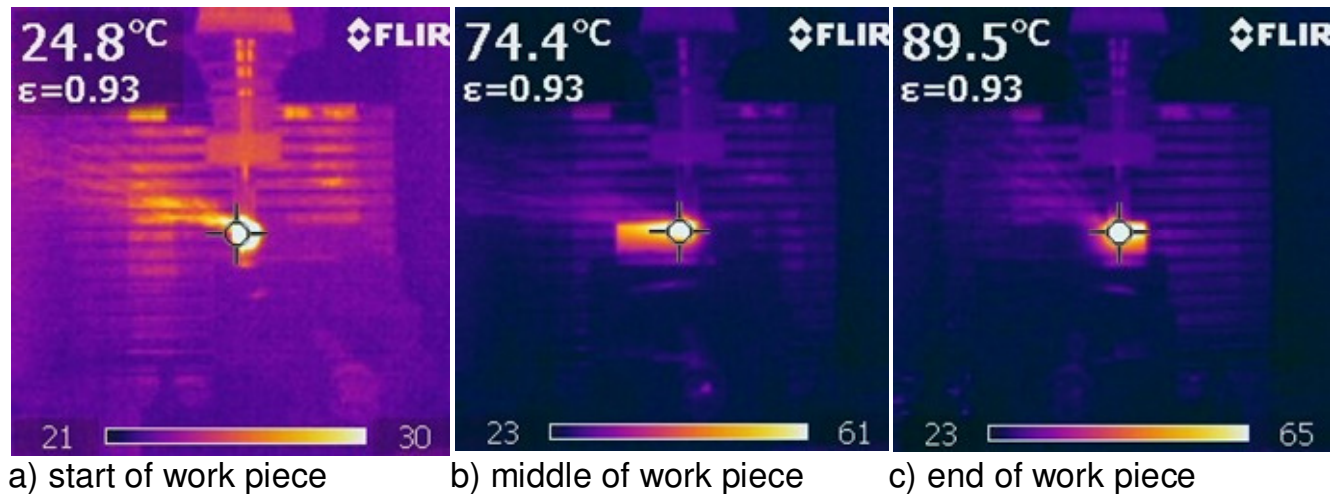


**Figure 2.** Thermograms showing the position of data acquisition.

border. The temperatures registered ranged from 23 to 65°C and the temperature peak was of 89.5°C. The symbol “ $\epsilon$ ” represents the emissivity of the work piece, which corresponds to 93% of the standard black body. The value for emissivity was considered 0.93 because it was necessary to paint the work piece with a black metallic spray covering all sides of the work piece.

Table 2 shows all temperature values in the milling experiments. Three replicas were carried out for each test and the data in Table 2 corresponds to average temperature values. The results demonstrate that independent of the number of thermograms and the feed rate, three medium values occur during the milling experiments along the axial direction of the end mill. These values represent temperatures at the top, middle, and bottom of the work piece along the axial direction of the end mill. Table 2 shows an increase in temperature for all milling conditions from the start to the end of the work piece. According to the results, we can say that the highest temperature in the work piece, considering the axial direction of the end mill, occurred in the middle of the work piece. At the top and bottom of the work piece, milling temperatures are lower due to the thermal heat exchange with the environment. All trials were carried out with a temperature of reference of  $23 \pm 1^\circ\text{C}$ .

The data analysis was performed using the software of the FLIR camera. This software allows you to find temperature values in recorded thermograms. The data of Table 2 provides a series of graphs that are shown in Figure 3. Specifically, Figure 3 represents the results of experiment number 11 and 12, where the three temperature positions for experiment number 11 and the five positions for experiment number 12 were recorded. Experiment number 11 used a feed rate of 0.1 mm/rev and 314 m/min of cutting speed as experimental factors. When we compare this with experiment number 12, which used a feed rate of 0.25 mm/rev, we can observe

that the increase in temperature was more significant in the first condition. In this case, the results show a strong relation of the feed rate with an increase in temperature. This occurred because of the long tool/work piece contact time when low feed rates are used. Thus, an accumulation of heat during the milling generates high heat flux in the work piece. For experiment number 11, a 140.5°C temperature peak can be observed and for experiment number 12 this peak was 88.1°C, showing a decrease of 59% in temperature.

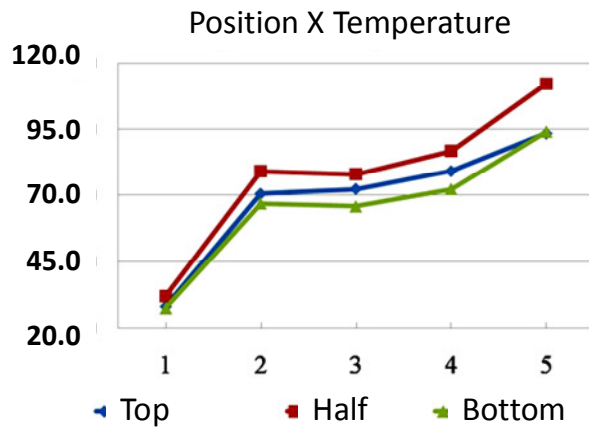
Figure 4 shows the influence of the radial depth of cut on temperature during end milling. Temperatures in both experiments were recorded in three positions. Experiment number 16 used a radial depth of cut of 2 mm and registered lower temperature values than experiment number 12. The second case demonstrates that the radial depth of cut has more influence on the end milling process when experiments with the same cutting speed and feed rate are compared. However, when we compare the two cases, we can observe that the low feed rate is more significant than the radial depth of cut, because the temperature peak in the latter case was 88.1°C at most.

Tables 3 and 4 summarize the temperature peaks for the two aforementioned cases. It can be affirmed that the more important experimental factor for an increase in temperature for these two milling conditions was the feed rate. One can observe that a long time of work piece/tool contact increased the temperature during the trial because of a low feed rate. The use of a low value for radial depth of cut and a high feed rate, therefore, produced the lowest temperature. This could have occurred because of the faster displacement of the tool associated with a small cutting section.

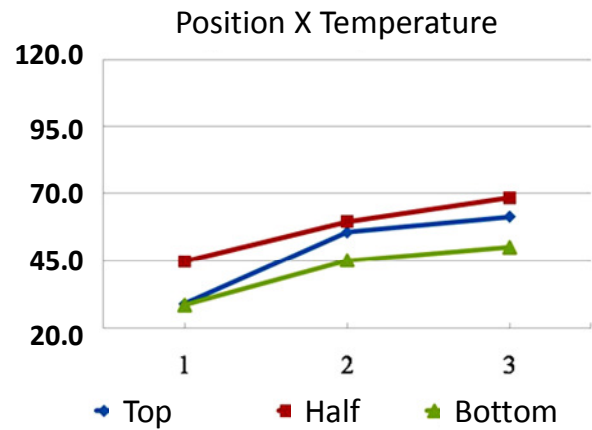
Figure 5 shows the experiments number 16 and 14, and one can note that the input parameters were constant except for the cutting speed of experiment number 14, which used a cutting speed of 628 m/min.

**Table 2.** Temperatures of the milling experiments.

Trial	$a_e$ (mm)	Vc(m/min)	Fz (mm/rev)	Cut direction	Average temperature (°C)				
					Start		Middle		End
1	6	628	0,1	Up-milling	33.0	60.2	70.5	67.6	94.5
					44.9	88.7	87.0	89.0	112.2
					37.4	63.6	63.1	64.5	71.5
2	6	628	0.25	Up-milling	47.3		69.0		76.0
					69.2		73.6		87.7
					51.9		66.1		71.1
3	6	314	0.1	Up-milling	56.4	77.1	88.7	81.5	107.5
					61.6	98.7	101.4	98.2	121.3
					46.6	79.1	81.7	80.6	102.7
4	6	314	0.25	Up-milling	63.6		71.1		75.0
					75.2		81.4		86.2
					58.7		69.4		66.6
5	2	628	0.1	Up-milling	44.9	84.0	70.8	68.7	96.0
					64.7	87.2	90.3	89.3	117.5
					50.6	77.4	78.2	78.0	96.6
6	2	628	0.25	Up-milling	50.6		56.8		61.0
					51.9		66.8		79.2
					45.8		53.6		65.0
7	2	314	0.1	Up-milling	47.7	70.3	73.2	72.9	82.8
					55.3	83.4	82.8	84.8	105.1
					45.7	65.5	70.9	68.0	90.4
8	2	314	0.25	Up-milling	29.3		62.0		61.4
					55.7		70.2		73.6
					35.0		59.0		56.8
9	6	628	0.1	Down-milling	35.8	72.1	80.3	81.3	107.1
					48.9	81.7	92.9	102.9	115.3
					42.5	73.4	71.8	78.2	91.8
10	6	628	0.25	Down-milling	55.5		78.8		87.8
					68.0		82.4		91.6
					58.6		75.5		73.9
11	6	314	0.1	Down-milling	39.8	90.7	92.8	101.1	118.2
					44.4	100.9	99.5	110.1	140.5
					39.0	86.3	85.0	92.7	118.8
12	6	314	0.25	Down-milling	40.8		72.8		79.7
					59.8		77.6		88.1
					40.4		60.2		66.3
13	2	628	0.1	Down-milling	53.3	90.5	89.1	87.3	120.2
					60.5	96.2	96.0	96.6	125.4
					47.1	81.8	85.2	87.2	105.3
14	2	628	0.25	Down-milling	54.9		61.3		61.3
					64.0		71.6		76.6
					56.0		61.9		56.9
15	2	314	0.1	Down-milling	41.4	74.6	82.1	88.6	101.6
					52.3	86.8	92.8	91.5	122.1
					41.8	76.9	75.7	79.9	97.4
16	2	314	0.25	Down-milling	49.5		63.5		67.5
					61.9		69.3		68.5
					53.0		59.4		58.2

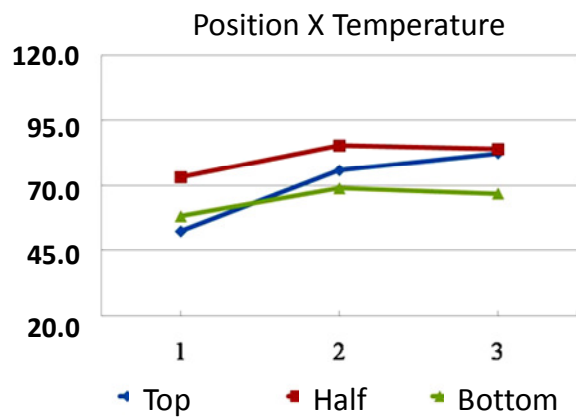


Trial number 11 ( $f_z=0.1\text{mm/rot}$ ,  $a_e=6\text{mm}$ ;  $V_c=314\text{m/min}$ )

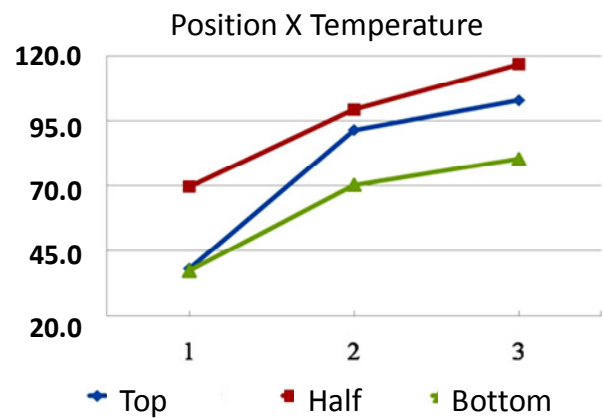


Trial number 12 ( $f_z=0.25\text{mm/rot}$ ,  $a_e=6\text{mm}$ ;  $V_c=314\text{m/min}$ )

Figure 3. Influence of feed rate on temperature during the end milling.



Trial number 16 ( $f_z=0.25\text{mm/rot}$ ,  $a_e=2\text{mm}$ ;  $V_c=314\text{ m/min}$ )



Trial number 12 ( $f_z=0.25\text{mm/rot}$ ,  $a_e=6\text{ mm}$ ;  $V_c=314\text{ m/min}$ )

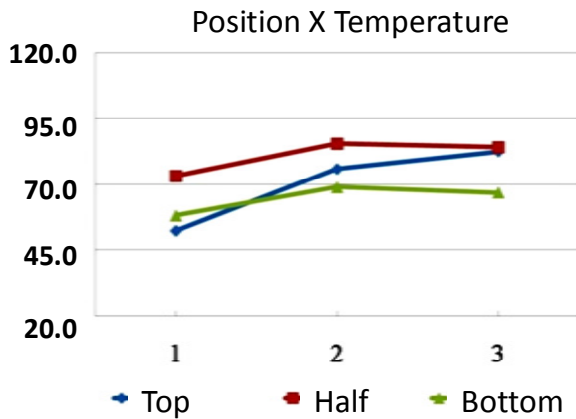
Figure 4. Influence of radial depth of cut on temperature during the end milling.

Table 3. Results of experiments number 11 e 12.

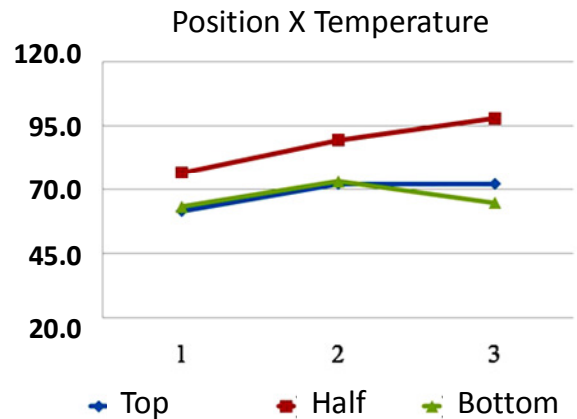
Trial number	Ae (mm)	Vc (m/min)	Fz (mm/rot)	Cut direction	Temperature peaks (°C)
11	6	314	0.10	Down-milling	140
12	6	314	0.25	Down-milling	89

Table 4. Results of experiments number 16 e 12 and, 16 and 14.

Trial number	Ae (mm)	Vc (m/min)	Fz (mm/rot)	Cut direction	Temperature peaks (°C)
<b>Number 16 e 12</b>					
16	2	314	0.25	Down-milling	67
12	6	314	0.25	Down-milling	89
<b>Number 16 and 14</b>					
16	2	314	0.25	Down-milling	67
14	2	628	0.25	Down-milling	76

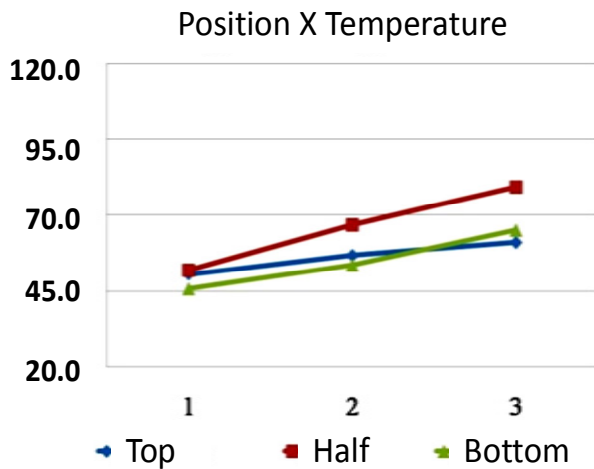


Trial number 16 ( $f_z=0.25$  mm/rot,  $a_e=2$ mm;  $V_c = 314$  m/min)

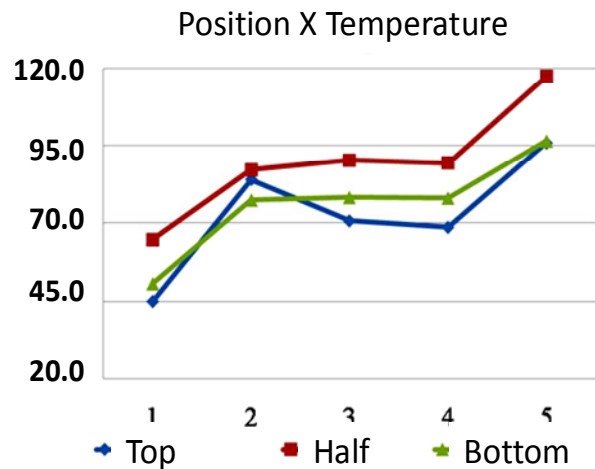


Trial number 14 ( $f_z=0.25$ mm/rot,  $a_e=2$ mm;  $V_c=628$  m/min)

Figure 5. Influence of cutting speed on temperature during the end milling.



Trial number 6 ( $V_c=628$ mm/min,  $a_e=2$ mm;  $f_z=0.25$  mm/rot)



Trial number 5 ( $V_c=628$ mm/min,  $a_e=2$ mm;  $f_z=0.1$  mm/rot)

Figure 6. Influence of cutting speed on temperature for up-milling using high cutting speed.

The temperature peak for experiment number 14 was 13% higher than for experiment number 16. It shows that the cutting speed has little influence on temperature in end milling processes, considering the parameters used for these trials. This demonstrates that by using constant input parameters and varying only the cutting speed, low temperatures can be achieved. This way, it can be supported that using high cutting speeds and high feed rates in the end milling process not only permits more production in less time, but also with low temperatures, avoiding high heat transfer to the work piece.

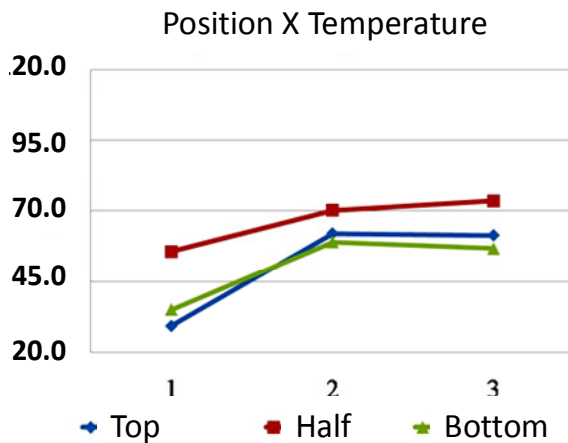
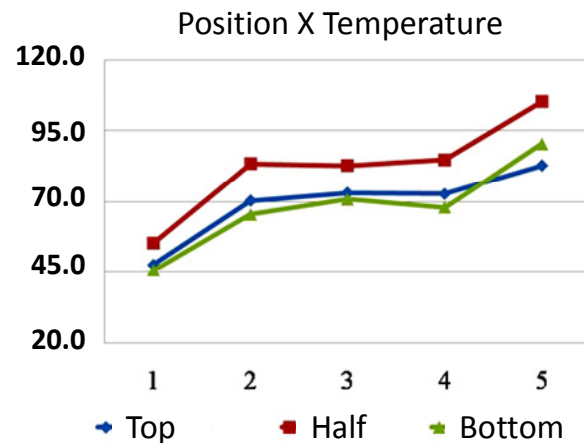
The third analysis evaluated four trials that were subdivided in two by two. Trials number 6 and 5 used a

radial depth of cut and feed rate of 2 mm and 0.25 mm/rev, respectively. Finally, trials number 8 and 7 used the same depth of cut of 2 mm with a feed rate of 0.10 mm/rev. Therefore, only the cutting speed varied during the experiments. This evaluation was considered because all tests were carried out in the up-milling direction, which according to the literature normally shows an increase in temperature.

Figure 6 shows the results of the trials number 6 and 5 with a variation of the feed rates. Comparing the results, we can observe that a temperature peak of 199°C occurred with a low feed rate for trial number 11. In the same way, when low cutting speeds are considered, we

**Table 5.** Results of trials number 6, 8, 5 and 7.

Trial number	ae (mm)	vc (m/min)	fz (mm/rot)	Cut direction	Temperature peaks (°C)
6	2	628	0.25	Up-milling	81
8	2	314	0.25	Up-milling	71
5	2	628	0.10	Up-milling	119
7	2	314	0.10	Up-milling	102

Trial number 8 ( $V_c=314$ mm/min,  $a_e=2$ mm;  $f_z=0.25$  mm/rot)Trial number 7 ( $V_c=314$ mm/min,  $a_e=2$ mm;  $f_z=0.1$  mm/rot)**Figure 7.** Influence of cutting speed on temperature for up-milling using low cutting speed.

can observe that the behavior was similar, with a temperature peak of 120°C. Table 5 shows a summary of the results of the four trials of the third case.

Figure 7 shows the results for trials number 8 and 7, which used a cutting speed of 314 m/min. It can be observed that, in the same way that occurred in trials number 6 and 5, a temperature peak occurred when the feed rate of 0.1 mm/rev was used. In summary, it can be supported that temperature peaks occurred when low feed rates were applied for those experimental conditions.

## DISCUSSION

Figures 3 to 7 show that the temperature increases for all conditions. According to the results it can be stated that high temperature peaks occurred when low feed rates were used. Thus, the most influent input parameter on temperature was feed rate. The temperature rises steadily with an increase in the cutting speed, but not as significant as with the feed rate.

The up-milling cutting direction did not generate higher temperature peaks than down-milling, contrary to what was expected. The cut area in milling increased from zero to the maximum when the up-milling direction was applied and in the opposite situation when down-milling

was applied. However, the cut direction did not cause great differences in temperature. The temperature variation was only 1°C with the change of cut direction. The drop in temperature that occurred from the upward to downward direction can therefore be considered to be negligible.

Considering the radial depth of cut, it can be supported that the temperature increases when the cut section increases. In machining process the temperature is directly related to the increase in area. According to Aspinwall et al. (2013), high cutting temperatures cause a drop in plastic yield strength, which results in easier cutting. The temperature increased from 71.4 to 77.3°C with a variation in radial depth of cut from 2 to 6 mm. The temperature dropped from 75.9 to 72.9°C with the increase of cutting speed.

The thermograph technique demonstrated great feasibility during the experimental tests. The interpretation and recording of temperature data in the data acquisition process proved to be easy. This enables quick decisions in real time during the supervision of the milling process. The cutting conditions, such as feed rate, cutting direction, cutting speed, and depth of cut, must therefore be selected in such a way that the predicted temperature does not exceed diffusion limits. Finally, a database can be generated connecting the infrared camera to a specific motherboard assembly on a

computer permitting access to the recorded information at some later time.

## Conclusions

According to the results presented in this paper, the following conclusions can be drawn:

1. The use of the thermograph technique has proven to be a powerful tool in monitoring machining processes, being feasible and easy to use;
2. Considering the input parameters, we can say that by using a low radial depth of cut, less variation of temperature occurred in the cutting region;
3. The cutting speed also provided temperature variation, but it was lower than the variation caused by the feed rate;
4. Feed rate represents the most significant input parameter to be controlled, because a high feed rate generated low heat flux in the work piece and the lowest temperature peaks;
5. When the cutting directions are compared, we can state that up-milling generates lower temperature peaks than down-milling in the milling of aluminum.

## AKNOWLEDGEMENTS

Sincere thanks to all who contributed to the present work, especially to Mr. Aldeci Santos -Sandvik Coromant – Brazil and Prof. Dr. Jefferson de Oliveira Gomes – Technological Institute of Aeronautics.

## REFERENCES

- Aspinwall DK, Mantle AL, Chan WK, Hood R, Soo SL (2013). Cutting temperatures when ball nose end milling  $\gamma$ -TiAl intermetallic alloys. CIRP Annals – Manufac. Tech., In Press.
- Biermann D, Heilmann M (2010). Improvement of workpiece quality in face milling of aluminum alloys. J. Mater. Proc. Technol. 210(14):1968-1975.
- Brandão LC, Coelho RT, Rodrigues AR (2008). Experimental and theoretical study of workpiece temperature when end milling hardened steels using (TiAl)N-coated and PcBN-tipped tools. J. Mat. Proc. Technol. 199(1/3):234-244.
- Chern G-Liang (2006). Experimental observation and analysis of burr formation mechanisms in face milling of aluminum alloys. Int. J. Mach. T. Manuf. 46(12/13):1517-1525.
- Davim JP, Correia AE (2006). Maquinagem a Alta Velocidade – Fresagem / CNC. Publindústria. No. 182.
- Davoodi B, Hosseinzadeh H (2012). A new method for heat measurement during high speed machining. Measurement 45(8):2135-2140.
- Dörr J, Mertens Th, Engering G, Lahres M (2003). 'In-situ' temperature measurement to determine the machining potential of different tool coatings. Surf. Coat. Tech. 174-175:389-392.
- Le Coz G, Marinescu M, Devillez A, Dudzinski D, Velnom L (2012). Measuring temperature of rotating cutting tools: Application to MQL drilling and dry milling of aerospace alloys. Appl. Theor. Eng. 36:434-441.
- Luchesi VM, Coelho RT (2012). An inverse method to estimate the moving heat source in machining process. Appl. Theor. Eng., 45-46:64-78.
- Maranhão C, Davim P (2010). Finite element modelling of machining of AISI 316 steel: Numerical simulation and experimental validation. Simul. Mod. Pract. Theory 18(2):139-156.
- Mayr J, Jedrzejewski J, Uhlmann E, Donmez MA, Knapp W, Härtig F, Wendt K, Moriwaki T, Shore P, Schmitt R, Brecher C, Würz T, Wegener K (2012). Thermal issues in machine tools. CIRP Ann. – Manuf. Technol. 61(2):771-791.
- Oguz Ç (2012). Tool-chip temperature simulation on high pressure jet assisted machining of Ti6Al-V4. Sci. Res. Essays 7(8):873-880.
- Sutter G, Faure L, Molinari A, Ranc N, Pina V (2003). An experimental technique for the measurement of temperature fields for the orthogonal cutting in high speed machining. Int. J. Mach. Technol. Manuf. 43(7):671-678.
- Zaghbani I, Songmene V (2009). A force-temperature model including a constitutive law for Dry High Speed Milling of aluminium alloys. J. Mater. Proc. Technol. 209(5):2532-2544.